Experimental study on post-fire behavior of precast concrete columns with efficient reinforcement

Haoming Xu [1], Congcong Xue [1], Min Yu [2, *], Jianqiao Ye [3, *]

[1] School of Intelligent Manufacturing and Smart Transportation, Suzhou City University, Suzhou 215104, China.
[2] School of Civil Engineering, Wuhan University, Wuhan 430072, China.
[3] School of Engineering, Lancaster University, Lancaster, LA1 4YR, UK.

Abstract: Previous studies have indicated that precast concrete columns reinforced by efficient reinforcement exhibit favorable static and seismic performance at room temperature; however, their post-fire mechanical behavior has not been thoroughly investigated. This study conducted residual mechanical performance tests on ten full-scale precast concrete columns reinforced by efficient reinforcement and five comparative ordinary reinforced concrete columns after exposure to fire. The study parameters included reinforcement forms, duration of fire exposure, and cross-sectional dimensions. Each column was subjected to the ISO 834 standard fire, allowed to cool, and then tested under axial compression. The experimental findings revealed that the connection regions of the precast concrete columns maintained adequate strength after fire, with failures predominantly observed in the non-connection areas. An increase in fire exposure duration resulted in a notable decline in the load-bearing capacity and stiffness of these columns. After exposure to fire, the precast concrete columns reinforced by cluster reinforcement exhibited higher load-bearing capacity, axial stiffness, and ductility compared to columns reinforced by large-diameter reinforcement, whose performance was comparable to that of the ordinary reinforced concrete columns. Based on the test results and existing calculation methods, a simplified approach that considers the effect of reinforcement forms was proposed to predict residual load-bearing capacity of precast concrete columns reinforced by efficient reinforcement after fire.

Keywords: Precast concrete columns; Efficient reinforcement; Cluster reinforcement; Large-diameter reinforcement; Post-fire; Residual load-bearing capacity

1 Introduction

Precast concrete structures require pre-manufacturing of concrete load-bearing components in a factory, which are then transported to the site for assembly or connection. Compared to cast-in-place concrete structures, precast concrete structures offer numerous advantages, including enhanced construction quality and efficiency, reduced costs, and environmental benefits, leading to their widespread global application.

A crucial issue of a precast structure is its connections that must be effective and safe when connecting precast components under various load conditions. Conventional connection zones in a precast concrete structure often face challenges such as a high number of closely spaced reinforcing bars, making installation difficult and compromising the quality of the pour. To address these issues, researchers have recently proposed two types of precast concrete columns with "efficient reinforcement"[1, 2]. One of them used large-diameter reinforcing bars instead of medium-diameter bars and grouted splice sleeve connections (see Figure 1~~Figure 1~~(b)). The other used small-diameter bars bundled in the regions along the four corners of the column, with longitudinal rebar lapping in grout-filled ducts that are surrounded by confining spiral stirrups (see Figure 1~~Figure 1~~ (c)). Existing research has shown that precast concrete columns reinforced by efficient reinforcement exhibit favorable static and seismic performance at normal environmental temperature[1-7]. However, studies on their performance under and after elevated temperature, such as a fire, are still very limited[8] and are required urgently.

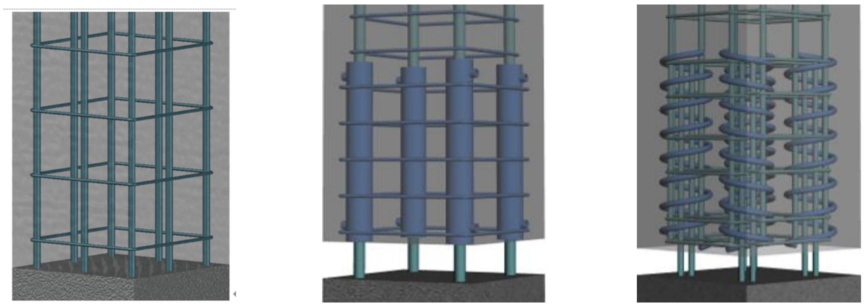

(a) Cast-in-place concrete column with normal reinforcement

(b) Precast concrete column with large-diameter rebars and sleeve grouting connections

(c) Precast concrete column with cluster reinforcement and constrained grouting-anchor connections

Figure 1 Conventional cast-in-place reinforced concrete column and precast concrete columns with efficient reinforcement

Fire is a frequent hazard for concrete structures, of which columns are normally vital load-bearing elements. Therefore, a systematic investigation of the mechanical properties of concrete columns after fire exposure is essential for the maintenance, reinforcement, and demolition of an engineering structure. Over the past few decades, a series of experiments on the mechanical properties of reinforced concrete columns after fire have been conducted by researchers such as Lie[9], Lin[10, 11], Jau[12], Chen[13], Wu[14], Zhang[15], Zhou[16], Bikhiet[17], Kodur[18], Abdulraheem[19, 20], Chen Jun[21, 22], Huo[23, 24], Vishal[25] and Lin X K [26]. Previous experimental studies suggested that concrete strength, aggregate type, section size, concrete cover thickness, reinforcement ratio, axial compression ratio, fire duration, fire exposure method, cooling method, and column end restraints were the main parameters that influenced residual performance of reinforced concrete columns after a fire. Jau et al.[12] demonstrated that a lower longitudinal reinforcement ratio resulted in a lower residual strength ratio of a column, while the longitudinal reinforcement ratio and the thickness of concrete cover did not affect the temperature distribution on the cross-sections of a column. Bikhiet et al.[17] found that larger diameter bars experienced greater transverse strain under high temperatures compared to smaller diameter bars, making concrete more prone to spalling, thus indicating that smaller diameter bars were more beneficial for enhancing residual load-bearing capacity of reinforced concrete columns after fire. Based on the experimental research, several simplified calculation methods for the residual strength of fire-exposed reinforced concrete columns have been reported[26-29]. Xu et al.[28] provided an empirical formula for calculating residual strength of square reinforced concrete columns after standard fire exposure. Kodur et al.[29] proposed a rapid evaluation method for residual strength of fire-exposed reinforced concrete columns, based on the 500°C isotherm method. While these methods account for various influencing factors, they have not sufficiently considered the impact of different reinforcement forms.

Most previous studies have focused on cast-in-place reinforced concrete columns, which typically have simple reinforcement forms and limited cross-sectional dimensions. Additionally, for precast concrete columns, the construction of the connection zone is complex, and the post-fire safety of the connection zone also needs experimental verification. Therefore, this paper conducted residual mechanical performance tests on ten full-scale precast concrete columns reinforced by efficient reinforcement and five relatively ordinary reinforced concrete columns after exposure to fire. The test variables included reinforcement forms, fire exposure duration, and cross-sectional size. The focus was on examining the cross-sectional temperature distribution, fire damage, failure modes, residual load-bearing capacity, axial stiffness, and ductility performance of the concrete columns after fire exposure. Subsequently, the applicability of existing simplified calculation methods to the columns tested in this paper was assessed. Finally, based on the 500°C isotherm method of Eurocode 2, a residual load-bearing capacity calculation method considering the impact of reinforcement forms was proposed for precast concrete columns reinforced by efficient reinforcement.

2 Experimental program

2.1 Description of the specimens

A total of 15 concrete columns were designed and fabricated for this experiment. The research parameters included column type, cross-sectional dimensions, and fire exposure duration. Table 1~~Table 1~~ presents the detailed design parameters. DS, CS, and RS refer to precast concrete columns with large-diameter reinforcement, precast concrete columns with cluster reinforcement, and conventional cast-in-place reinforced concrete columns, respectively. B350, B400, and B450 denote square column cross-sections with side lengths of 350 mm, 400 mm, and 450 mm, respectively. T60, T90, and T120 indicate the columns' exposure times to fire of 60 minutes, 90 minutes, and 120 minutes, respectively.

Table 1 Summary of the tested columns

Column reference	Column type	Longitudinal steel bars		Section dimensions/ mm×mm	Fire duration (min)
		Number and diameter (mm)	Reinforcement ratio (%)		
DS-B400-T60	Precast concrete column with large diameter rebars and sleeve grouting connections	4Ø28	1.54		60
DS-B400-T90		4Ø28	1.54	400×400	90
DS-B400-T120		4Ø28	1.54		120
DS-B350-T90		4Ø28	2.01	350×350	90
DS-B450-T90		4Ø28	1.22	450×450	90
CS-B400-T60	Precast concrete column with cluster reinforcement and constrained grouting-anchor connections	16Ø14	1.54		60
CS-B400-T90		16Ø14	1.54	400×400	90
CS-B400-T120		16Ø14	1.54		120
CS-B350-T90		16Ø14	2.01	350×350	90
CS-B450-T90		16Ø14	1.22	450×450	90
RS-B400-T60	Conventional cast-in-place reinforced concrete column	8Ø20	1.57		60
RS-B400-T90		8Ø20	1.57	400×400	90
RS-B400-T120		8Ø20	1.57		120
RS-B350-T90		8Ø20	2.05	350×350	90
RS-B450-T90		8Ø20	1.24	450×450	90

Each specimen was 2020 mm in height. The reinforcement grade was HRB400, and the concrete grade was C40. High-strength, non-shrink grout was used for the reinforcement connections in the precast columns. Figure 2~~Figure 2~~ illustrates the reinforcement details and other specifics. The precast columns consisted of two parts: the upper part served as the test segment with a designed length of 1500 mm, and the lower part simulated the beam-column joints in practical engineering design, with a designed length of 500 mm. A 20 mm thick layer of grout was placed between the upper and lower parts. Stirrups were constructed using 8 mm diameter HRB400 steel bars. To facilitate hoisting and loading, steel end plates measuring 560 mm × 600 mm × 20 mm were installed at both ends of the columns.

Formatted: Font: (Asian) SimSun

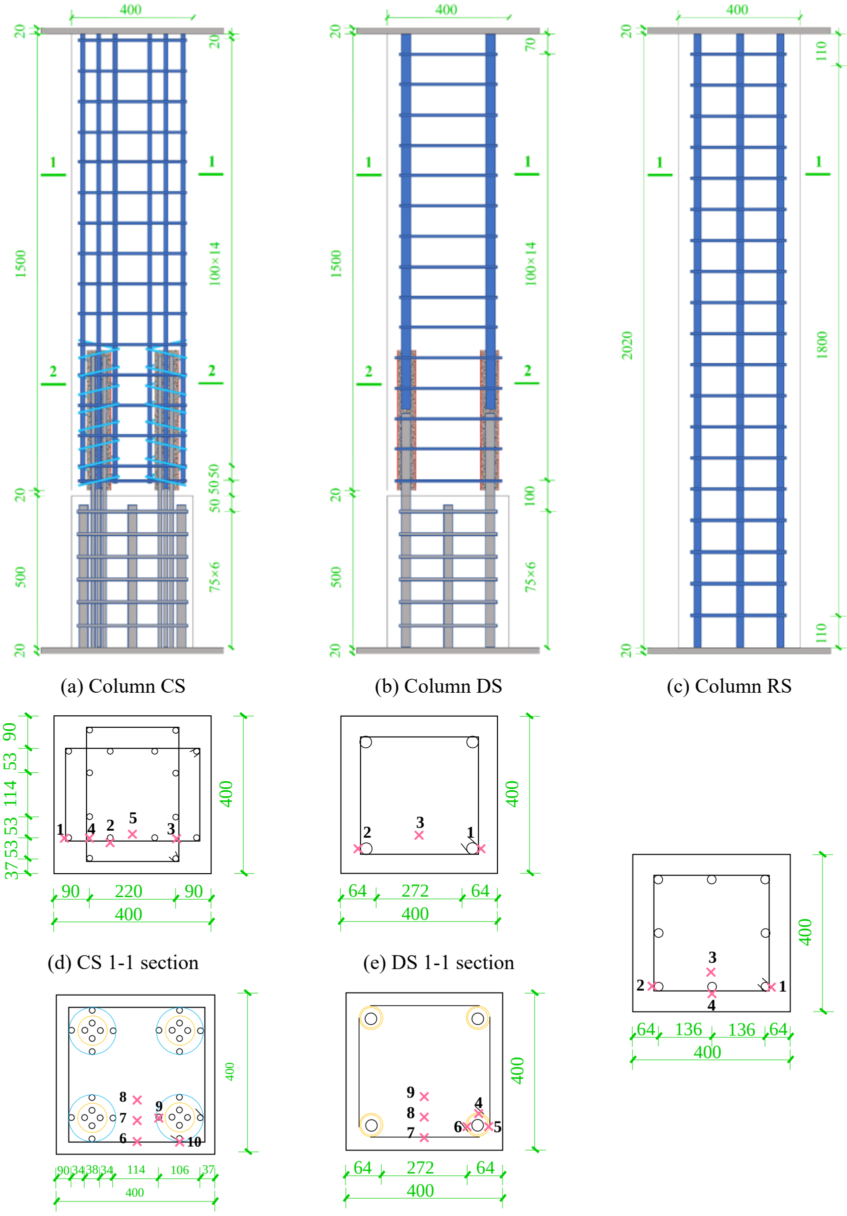

(a) Column CS (b) Column DS (c) Column RS

(d) CS 1-1 section (e) DS 1-1 section

(f) CS 2-2 section (g) DS 2-2 section (h) RS 1-1 section

Figure 2 The elevation, cross-section details and thermocouple arrangement of the specimens (mm)

2.2 Specimen preparation

The manufacturing process of the specimens was as follows: (1) Rebar Cage Preparation: The rebar cage was tied according to the design specifications. Mortar spacers of the same thickness as the concrete cover were used to position the rebar cage within the mold. Steel plates were welded to the ends of the longitudinal bars, and sleeves, steel pipe inserts, and thermocouples were positioned within the rebar cage. The sealing and stability of the mold were checked (Figure 3~~Figure 3~~(a)-(c)). (2) Concrete Casting and Curing: Concrete was cast and cured for 15 days. (3) Assembly of Precast Column Segments: The upper and lower parts of the precast columns were assembled by inserting the protruding rebar from the lower part into the sleeves or reserved holes (Figure 3~~Figure 3~~(d)). Quick-setting cement mortar was used to seal the joint surface. After 12 hours, the sleeves and holes were grouted (Figure 3~~Figure 3~~(e)). (4) Curing and Drying: The specimens were further cured with water for 28 days, followed by natural drying (Figure 3~~Figure 3~~(f)). More details about the specimen manufacturing process can be found in reference[8].

Type K thermocouples with a diameter of 3 mm were used. Temperature measurement points were primarily located on the rebar, the surface of the sleeves, and at various depths within the concrete. The concrete mix proportion, i.e., the ratio of water: cement: sand: aggregate: water reducer is 140: 360: 850: 1045: 5 (kg/m³). During the fire exposure tests, the average compressive strengths of the concrete and the grout were 46.4 MPa and 96.4 MPa, respectively. The yield strengths of the 14 mm, 20 mm, and 28 mm longitudinal bars were 510 MPa, 475 MPa, and 464 MPa, respectively, with ultimate strengths of 625 MPa, 602 MPa, and 605 MPa. The yield strength and ultimate strength of the stirrups were 423 MPa and 576 MPa, respectively.

(a) Reinforcement cage of column CS   (b) Reinforcement cage of column DS   (c) Reinforcement cage of column RS

(d) Assembling   (e) Grouting   (f) Natural curing

Figure 3 Specimen production process

2.3 Fire exposure test

The fire exposure tests were conducted using a high-temperature electric furnace in the Structural Engineering Laboratory at Wuhan University, as illustrated in Figure 4~~Figure 4~~. The furnace comprised four main components: the heating chamber, temperature control system, ventilation system, and data acquisition system. The heating chamber accommodated specimens with maximum cross-sectional dimensions of 500mm × 500mm and reached a maximum temperature of 1200°C. The heating length of each specimen was 1500mm.

Formatted: Font: (Asian) SimSun

To prevent damage to the furnace from concrete spalling during fire exposure, the specimen surfaces were covered with steel wire mesh. The furnace utilized a three-zone temperature control system (top, middle, and bottom). The temperature control system automatically adjusted the temperature according to a pre-set heating and cooling curve. Temperature data were collected using an AT4516 multi-channel temperature data logger, which measured temperatures at up to 48 points simultaneously with an accuracy of ±0.3°C.

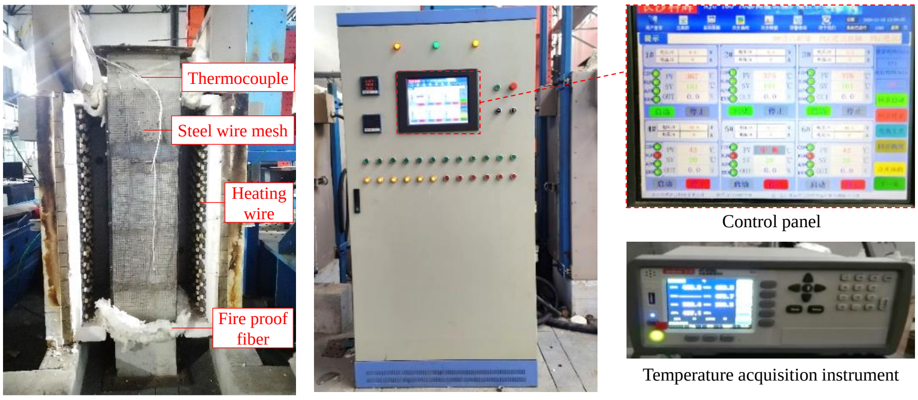

(a) Internal view of the high-temperature electric furnace

(b) Temperature control and acquisition devices

Figure 4 Fire testing setup

The tests followed the ISO-834 standard heating and cooling curve[30], as shown in Figure 5~~Figure 5~~(a). The measured furnace temperature is presented in Figure 5~~Figure 5~~(b), indicating that the furnace temperature followed closely the ISO-834 standard fire curve.

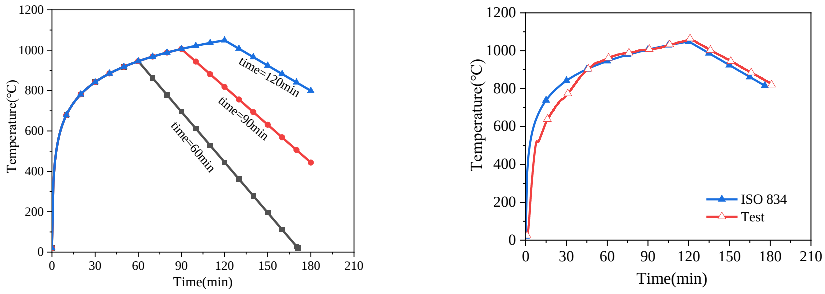

(a) ISO-834 standard fire curve

(b) Measured furnace temperature

Figure 5 Temperature profile and measured furnace temperature

2.4 Mechanical testing setup and procedure

After each column was fully cooled to ambient temperature after the fire exposure, the damage of the columns was carefully inspected. Subsequently, mechanical performance tests were conducted at the Structural Engineering Laboratory of Wuhan University. The test setup and specimen loading are shown in Figure 6~~Figure 6~~. A 3000-ton compression testing machine was used for axial loading (Figure 6~~Figure 6~~(a)). Column deflections at several locations were recorded using linear variable differential transducers (LVDT), and the data were collected with a DH3816 static strain acquisition system.

The installation and loading procedure for the specimens included the following steps: (1) The test columns

Formatted: Font: (Asian) SimSun

Formatted: Font: (Asian) SimSun

were vertically aligned and centered with the compression testing machine (Figure 6~~Figure 6~~(c)). (2) Four LVDT were placed at the four corners of the column's top end and connected to the strain acquisition system. (3) Displacement-controlled loading was applied at a rate of 0.6 mm/min. The loading process terminated when the load capacity dropped to 50% of the peak load, marking the end of the test.

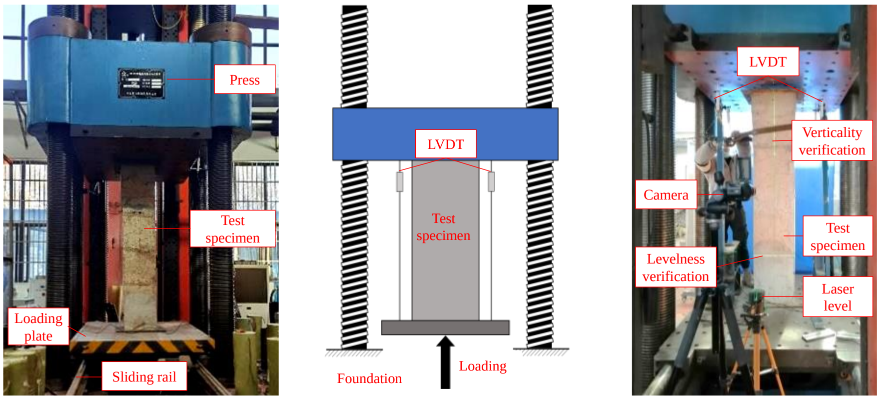

(a) 3000-ton capacity testing machine

(b) Axial compression loading diagram

(c) Specimen installation

Figure 6 Residual mechanical performance testing setup

3 Experimental results

During the heating process, the first audible concrete spalling sounds were heard within 10 to 15 minutes of fire exposure, when the furnace temperature was approximately 600°C. The spalling generally ceased after about 30 minutes of heating. After about 20 to 30 minutes of fire exposure, steam began to exit from the top of the furnace (Figure 7~~Figure 7~~(a)), and water was observed flowing down from the heated section of the column (Figure 7~~Figure 7~~(b)). As the furnace temperature continued to rise, the steam became increasingly dense, gradually disappeared during the cooling phase. The steam observed during the heating process originated from the evaporation and migration of moisture within the concrete due to the high temperature. The combination of steam pressure and temperature gradient was the primary cause of spalling in the concrete cover during the early stages of heating. As the temperature gradient and moisture content in the concrete cover sharply decreased afterward, no noticeable spalling was observed.

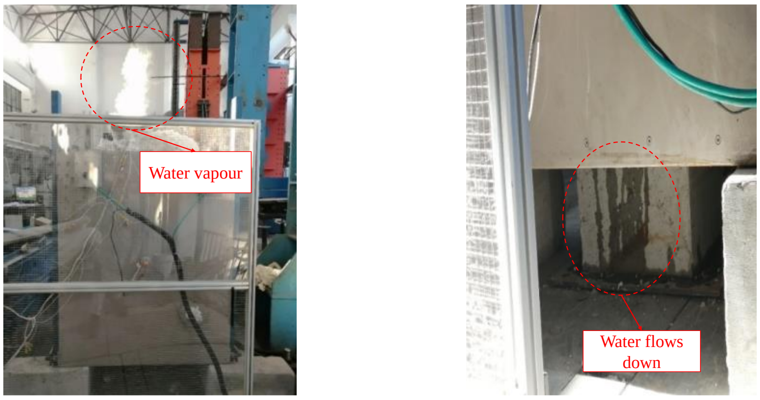

(a) Water vapour above furnace

(b) Water flowed down from the fire-exposed

Formatted: Font: (Asian) SimSun

Commented [JY1]: Am I right? Not after. Maay be after fire started?

Commented [hx2R1]: Yes. The concrete spalling sounds occurs during the process of columns being exposed to fire.

Formatted: Font: (Asian) SimSun

Formatted: Font: (Asian) SimSun

section of the column

Figure 7 Experimental phenomena in fire exposure

3.1 Fire exposure tests results

3.1.1 Thermal response

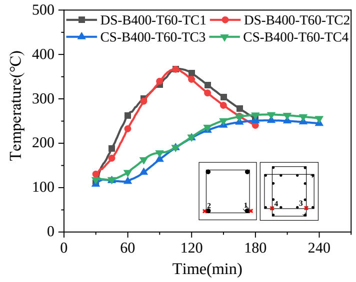

(a) Same depth of measurement points

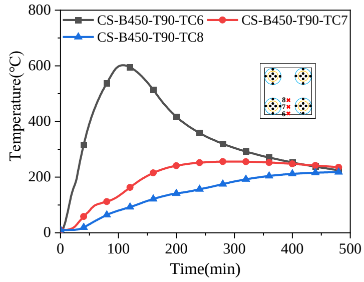

(b) Different depths of measurement points

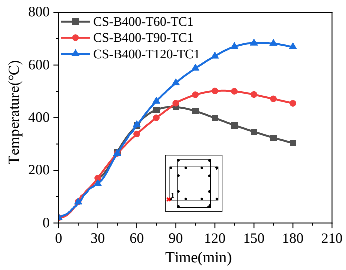

(c) Different fire exposure times

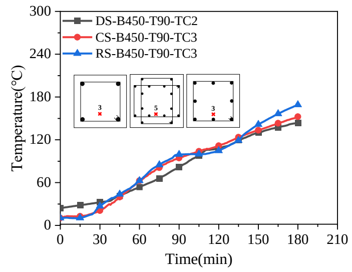

(d) Different reinforcement forms

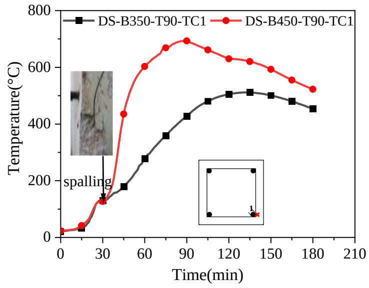

(e) The effect of spalling

Figure 8 Measured temperatures as a function of time in the tested columns

The comparison of the temperatures recorded at symmetric points within the precast concrete columns is shown in Figure 8~~Figure 8~~(a). It was observed that measuring points 1 and 2 on column DS-B400-T60 were symmetrically placed on the surface of the large-diameter longitudinal reinforcement, and both reached a maximum temperature of 367°C. The time required to reach this peak temperature was 107 minutes and 104 minutes, respectively. For column CS-B400-T60, measuring points 3 and 4 were symmetrically located at the center of the cross-section of the bundled longitudinal reinforcement. A maximum temperature of 251°C and 264°C, respectively, were reached after 190 minutes heating. The consistent temperature change at symmetrically arranged measuring points during fire exposure indicated a uniform temperature distribution within the furnace.

Taking specimen CS-B450-T90 as an example, the temperature-time curves for different depths within the cross-section of the precast concrete column are shown in Figure 8~~Figure 8~~(b). Measurement points 6, 7, and 8 were positioned along the central axis of the cross-section at varying depths. The maximum temperatures recorded at these points were 602°C, 256°C, and 218°C, respectively, which occurred respectively at 109 minutes, 298 minutes, and 480 minutes. Compared with the time when the furnace reached its maximum temperature, the above times were 21%, 231%, and 433% longer, respectively. It was evident that the deeper the measurement point was located, the lower the maximum temperature was, and the longer it took to reach it. This longer time was primarily attributed to the low thermal conductivity, high specific heat capacity, and significant thermal inertia of concrete.

The influence of different fire exposure durations on the cross-sectional temperature of the precast columns is shown in Figure 8~~Figure 8~~(c). Measurement point 1 was located at the outermost longitudinal reinforcement of the section. After 60 minutes, 90 minutes, and 120 minutes of fire exposure, the maximum temperatures recorded at point 1 for the three precast columns with cluster reinforcement were 440°C, 502°C, and 684°C, respectively. It was observed that a longer fire exposure duration~~s~~ resulted in a higher maximum temperature~~s~~ at the measurement points on the column section. When the fire exposure time exceeded 90 minutes, the ~~experienced~~ maximum temperature of the longitudinal bars exceeded 500°C, and their residual strength began to decrease[29].

The influence of different reinforcement methods on the cross-sectional temperature of the columns is illustrated in Figure 8~~Figure 8~~(d). The measurement points were located at 1/4L from the column edge (where L is the side length of the section). The figure shows that the temperature differences at the measurement points among the three types of reinforced columns were not significant during the fire exposure, indicating that the reinforcement method had little effect on the cross-sectional temperature. This small difference is attributed to the similar reinforcement ratios of the three sections and the small cross-sectional area occupied by the reinforcement, which was only 1.22%. Consequently, the reinforcement method did not significantly influence the temperature distribution across the section.

The impact of spalling on the temperature of precast concrete columns is shown in Figure 8~~Figure 8~~(e). Measurement point 1 on columns DS-B350-T90 and DS-B450-T90 was positioned at the same location, while the measured maximum temperatures under the same heating conditions differed by nearly 200°C. This discrepancy was primarily due to localized spalling of the concrete near measurement point 1 on the DS-B450-T90 column during heating, which reduced the distance from the point to the fire-exposed surface. As a result, the heating rate at this point increased, leading to a higher maximum temperature and a shorter time to reach it.

3.1.2 Damage of the precast columns after fire

Taking the specimen exposed to fire for 60 minutes as an example, its typical damage is shown in Figure 9~~Figure 9~~. The surface of the column displayed an overall grayish-white color, with localized areas appearing light red (Figure 9~~Figure 9~~(a)). Partial concrete spalling was evident, which predominantly concentrated along the column edges (Figure 9~~Figure 9~~(b)). The cracks on the column surface were short and fine, with more cracks observed near the edges, extending along the adjacent faces (Figure 9~~Figure 9~~(c)).

(b) Surface spalling

(a) General view (c) Surface cracks

Figure 9 Damage results of column DS-B400-T60 after fire exposure

The damage of the specimen exposed to fire for 120 minutes is shown in Figure 10~~Figure 10~~. Upon opening the furnace, a significant amount of concrete debris was found around the column. The concrete surface of the specimen generally exhibited a light reddish color. One of the four exposed surfaces of the column experienced a full-depth spalling of the surface concrete, with the maximum spalling depth reaching approximately 25mm (Figure 10~~Figure 10~~ (a)(b)). Numerous cracks were observed on the column surface, many of which were interconnected (Figure 10~~Figure 10~~ (c)).

Formatted: Font: (Asian) SimSun

Formatted: Font: (Asian) SimSun

Formatted: Font: (Asian) SimSun

(b) Surface spalling

(a) General view (c) Surface cracks

Figure 10 Damage results of column RS-B400-T120 after fire exposure

Based on the damage characteristics observed in the columns after fire exposure, the surface color of the specimens turned grayish-white after 60 minutes of fire exposure. As the exposure time increased to 120 minutes, the surface color changed to a light reddish hue. A large number of cracks appeared on the surface of the specimens, with edge cracks primarily oriented transversely and extending toward the center of the adjacent faces. With the increased duration of fire exposure, these surface cracks transitioned from being short and narrow to wide and long, with many becoming interconnected. The texture of the concrete gradually became more porous, and after 120 minutes of fire exposure, the concrete could be easily crushed by hand.

The spalling behavior of the specimens after fire exposure is summarized in Table 2~~Table 2~~. There was a significant correlation between the severity of concrete spalling and the duration of steam release during the fire. Specimens that exhibited intense and prolonged steam release generally experienced severer spalling. The spalling was primarily concentrated at the edges of the specimens, which is likely due to the higher temperatures and thermal stresses at the edges of square components exposed to fire on all sides, making them more prone to spalling. Unlike precast concrete columns, which only exhibited localized spalling, the ordinary concrete columns experienced full sectional spalling in the fire-exposed region. This difference is likely due to the higher moisture content in ordinary concrete columns, which were exposed to rainwater during outdoor curing, leading to severer spalling. These observations suggest that the spalling and crack distribution in concrete columns after fire exposure were not significantly influenced by cross-sectional dimensions or reinforcement patterns.

Table 2 Statistical table of spalling of each column

Column reference	Spalling location	Total Spalling Volume (cm³)
DS-B400-T60	Two at the edge	190
DS-B400-T90	Four at the edge	833
DS-B400-T120	One in the upper part	456
DS-B350-T90	No spalling	0
DS-B450-T90	Two at the edge and one in the middle part	2089
CS-B400-T60	Three at the edge	352
CS-B400-T90	One at the edge	263
CS-B400-T120	Seven at the edge and one in the upper part	4047
CS-B350-T90	One at the edge	414
CS-B450-T90	One at the edge	93
RS-B400-T60	Two full surfaces in the heated area	17870
RS-B400-T90	Two full surfaces in the heated area	10520
RS-B400-T120	One full surface in the heated area	5200
RS-B350-T90	Four at the edge	3846
RS-B450-T90	Three at the edge and one in the upper part	2593

3.2 Mechanical tests results

3.2.1 Failure process and final form

The typical failure process of precast concrete columns under axial compression after a fire is illustrated in Figure 11~~Figure 11~~. Taking column CS-B350-T90 as an example, during the initial loading phase, both the reinforcement and concrete remained in the elastic stage, and no noticeable changes were observed on the surface of the column (Figure 11~~Figure 11~~(a)). When the load reached approximately 83% of the peak load, the first visible longitudinal crack appeared at the location of the vertical reinforcement near the lower part of the sleeve; as the load continued to increase, the crack rapidly propagated downward and widened (Figure 11~~Figure 11~~(b)). Approaching the peak load, multiple vertical cracks rapidly developed on the column surface, widened quickly and accompanied by minor concrete spalling (Figure 11~~Figure 11~~(c)). After reaching the peak load, i.e., when

Formatted: Font: (Asian) SimSun

Formatted: Font: (Asian) SimSun

Formatted: Font: (Asian) SimSun

Formatted: Font: (Asian) SimSun

the bearing capacity dropped to approximately 0.9 times the peak load, vertical chunks of concrete detached from the column surface. The middle portion of the column bulged outward, horizontal cracks appeared, and the concrete was crushed, resulting in column failure (Figure 11~~Figure 11~~(d)).

Formatted: Font: (Asian) SimSun

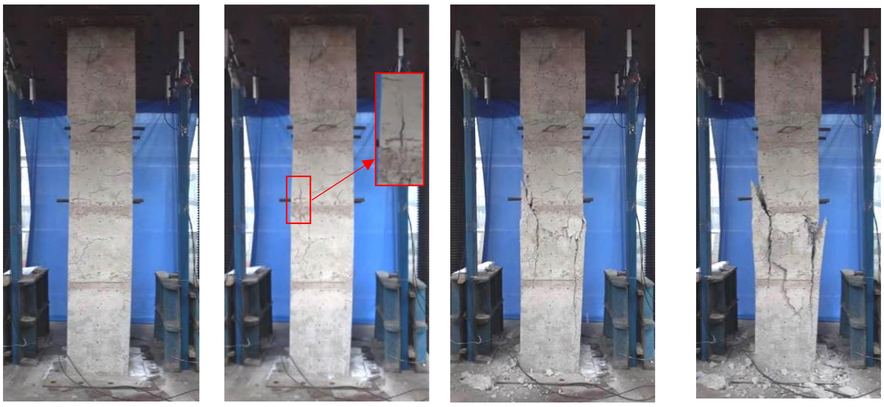

(a) Initial loading stage (b) First crack appears (c) Peak load reached (d) Failure

Figure 11 Failure process of precast concrete columns

Figure 12~~Figure 12~~~Figure 14~~Figure 14~~, respectively, illustrate the failure modes of the axial compression tests on the three types of columns after fire exposure. From these figures, all columns exhibited axial compression failure after the fire. The core concrete at the failure location was crushed and bulged outward, the longitudinal reinforcement yielded and locally buckled, the stirrups were deformed outward due to compression, and the concrete cover severely cracked and spalled. The precast concrete columns with efficient reinforcement demonstrated good performance in the connection zones after the fire, with no premature failures in these areas that could have compromised the overall structural integrity. Unlike the failure modes observed under room temperatures, the location of compression cracks in the columns after fire exposure was related to fire damage. Regardless of the reinforcement type, the longer the exposure time, the greater the initial damage, leading to earlier appearance of compression cracks on the column surface after the fire. For the same fire exposure duration, compression cracks appeared earlier in the precast concrete columns with cluster reinforcement compared to those with larger diameter reinforcement, but the crack propagation was slower, resulting in a more gradual failure.

Formatted: Font: (Asian) SimSun

Formatted: Font: (Asian) SimSun

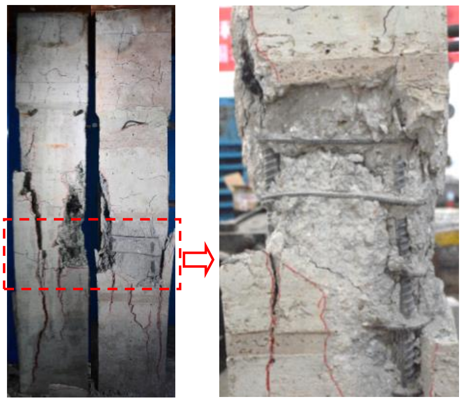

(a) General view (b) Crush and buckling

Figure 12 Failure mode of precast concrete column with large-diameter reinforcement

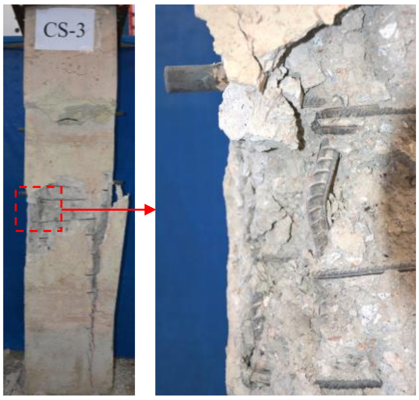

(a) General view (b) Local buckling

Figure 13 Failure mode of precast concrete column with cluster reinforcement

(a) General view (b) Concrete crushing

Figure 14 Failure mode of ordinary reinforcement concrete column

3.2.2 Analysis of load-deformation curve

The load-deformation curves for the concrete columns, obtained from the experiments, are shown in Figure 15~~Figure 15~~. The curves reveal distinct patterns with respect to increased fire exposure duration and cross-sectional size. Generally, as the fire exposure duration increased, the initial slope of the load-deformation curve decreased, the peak load reduced, the deformation corresponding to the peak load increased, and the post-peak curve exhibited a more gradual decline. Notably, for columns RS-B400-T60 and RS-B400-T90, the peak load unexpectedly increased with longer fire exposure. This was attributed to the severer concrete spalling observed in these columns (as shown in Table 2~~Table 2~~). The influence of increased cross-sectional size on the load-deformation curves demonstrated an opposite trend to that observed with fire exposure duration.

Formatted: Font: (Asian) SimSun

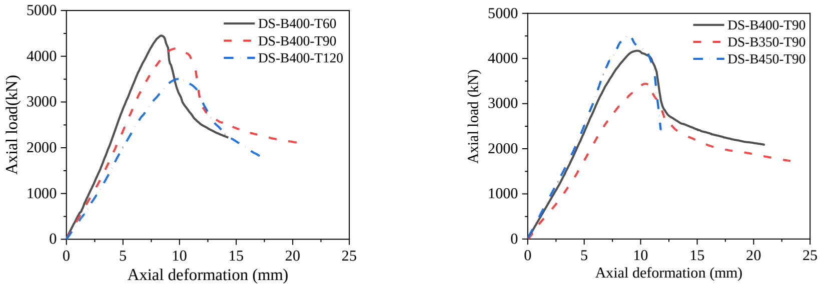

(a) Precast concrete column with large-diameter reinforcement

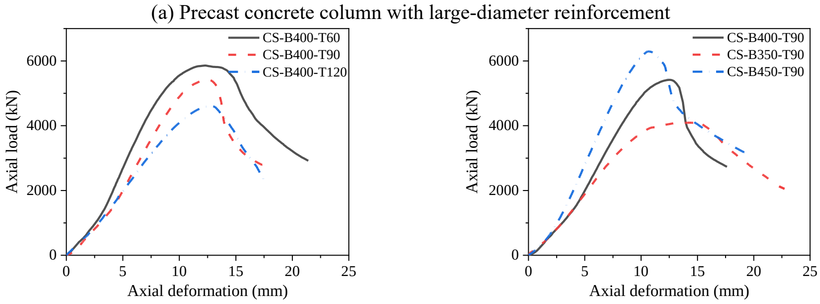

(b) Precast concrete column with cluster reinforcement

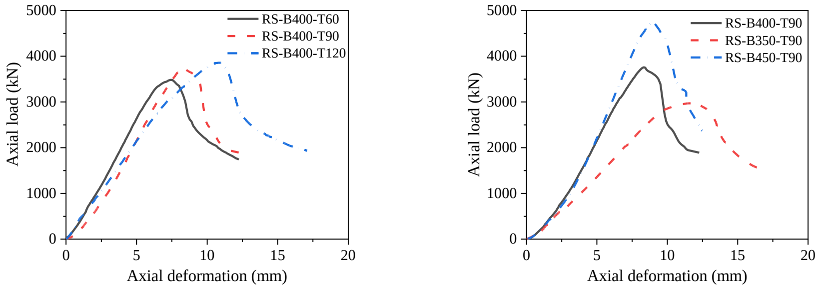

(c) Ordinary reinforced concrete column

Figure 15 Residual load-deformation response of the test columns

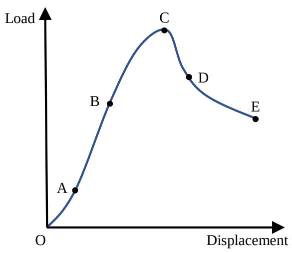

Figure 16 Typical load-deformation curve of precast concrete columns with efficient reinforcement

By studying the load-displacement curves of the specimens, typical load-deformation curves for axial compression of precast concrete columns with efficient reinforcement after high temperature can be obtained, as shown in Figure 16~~Figure 16~~. From the figure, the curve can be roughly divided into the following five stages, i.e., the stiffness strengthening stage, elastic stage, elastic-plastic stage, failure stage and residual stage of the specimen under axial compression, respectively.

Formatted: Font: (Asian) SimSun

(1) The ~~S~~stiffness strengthening stage (Segment OA): The load-deformation curve exhibits a slight concave upward shape, with a gradually increasing slope, indicating a stiffening stage. Due to the high temperature exposure, many micro-pores were generated inside the concrete after evaporation of internal moisture, and certain vertical expansional deformation occurred during the high-temperature heating process. Under the action of the load, the internal pores and micro-cracks of the column were initially compacted, resulting in an increase in the stiffness of the column.

(2) The ~~E~~elastic stage (Segment AB): At this stage, both the concrete and the steel bars were in the elastic stage, and the increase in compressive deformation of the column was proportional to the increase in load, resulting in linear relationship of the load-displacement curve.

(3) The ~~E~~elastic-plastic stage (Segment BC): As the load increased, cracks began to appear on the surface of the concrete and continued to propagate due to the development of plastic deformation in the concrete. The rate of compression deformation in the concrete increased faster than the rate of increase in load. This was manifested by a gradual flattening of the load-deformation curve.

(4) The ~~F~~failure stage (Segment CD): After surpassing the peak load, significant longitudinal cracks appeared around the column. The concrete cover failed, causing the longitudinal bars in the hoop to gradually buckle outward. The concrete was crushed, leading to a rapid decrease in load. This was manifested by a steep decline in the load-deformation curve.

(5) The ~~R~~residual stage (Segment DE): At this stage, the longitudinal bars and the outer concrete cover ceased to function, leaving only the core concrete to bear the load. Axial deformation continued to increase with ~~, while the load~~ slowly decreasing axial force~~ed~~.

4 Residual mechanical behavior

4.1 Residual load-bearing capacity

After exposure to high temperatures, the load-bearing capacity of the concrete columns was reduced due to the reduction in the material's mechanical properties. The residual load-bearing capacity of the specimens was derived from the load-deformation curves obtained during axial compression tests.

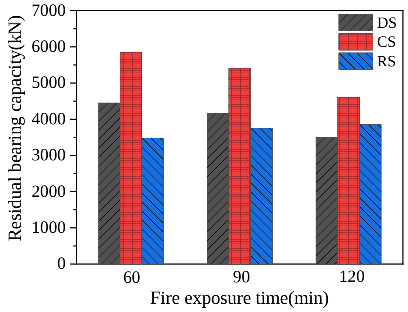

Figure 17 Effect of fire exposure duration on residual load-bearing capacity

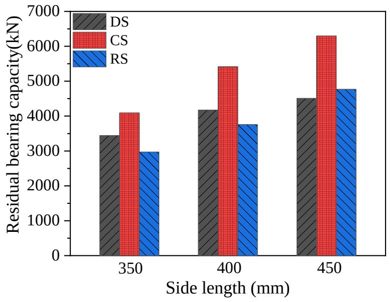

Figure 18 Effect of cross-sectional dimension on residual load-bearing capacity

Figure 17~~Figure 17~~ illustrates the impact of fire exposure duration on the residual load-bearing capacity of the concrete columns. As shown in the figure, the residual axial load-bearing capacity of the precast concrete columns decreased with the increase of duration of fire exposure. For the columns with a cross-sectional side

Formatted: Font: (Default) Times New Roman, (Asian) SimSun length of 400 mm, compared to those exposed to fire for 60 minutes, the residual capacity of the precast concrete columns with large-diameter reinforcement was decreased by 6% and 21% after 90 and 120 minutes of fire exposure, respectively. Similarly, the residual capacity of the precast concrete columns with cluster reinforcement was decreased by 8% and 21% after 90 and 120 minutes of fire exposure, respectively. It is evident that the rate of reduction was comparable between the two reinforcement configurations. The post-fire strength of steel and concrete is dependent on the maximum temperature they have reached. A higher temperature results in a greater reduction in the strength. Thus, as fire exposure time increases, the overall temperature of the cross-section is higher, leading to a decrease in the strength of both the steel and concrete, and consequently, a reduction in the residual load-bearing capacity of the precast concrete columns. In contrast, the ordinary reinforced concrete columns exhibited significant spalling after fire exposure. The volume of spalled concrete of RS-B400-T60 was greater than that of RS-B400-T90, and RS-B400-T120 had the smallest volume of concrete spalling (see Table 2~~Table 2~~). The spalling reduced the load-bearing area of the columns and altered the load application from axial to eccentric compression, further exacerbating the loss of load-bearing capacity. Ultimately, the reduction in load-bearing capacity caused by spalling exceeded that caused by prolonged fire exposure, leading to an observed increase in residual load-bearing capacity of the columns subjected to a longer fire exposure duration.

Figure 18~~Figure 18~~ shows the effect of cross-sectional size on the residual load-bearing capacity of the concrete columns. It was observed that, after the same fire exposure duration, an increase in cross-sectional size resulted in a higher residual load-bearing capacity. After 90 minutes of fire exposure, comparing with the specimen with cross-sectional side lengths of 350 mm, the residual load-bearing capacity of the precast concrete columns reinforced by large-diameter reinforcement with cross-sectional side lengths of 400 mm, and 450 mm were increased by 21% and 31%, respectively. Similarly, the residual load-bearing capacity of the precast concrete columns with cluster reinforcement were increased by 32% and 54%, while that of the ordinarily reinforced concrete columns were increased by 26% and 61%. These findings indicate that, for both types of precast concrete columns reinforced by efficient reinforcement, the increase in cross-sectional size has a more significant impact on the residual load-bearing capacity of the precast concrete columns reinforced by cluster reinforcement after fire exposure.

The effect of reinforcement configuration on the residual load-bearing capacity of concrete columns is also evident in Figure 17~~Figure 17~~ and Figure 18~~Figure 18~~. In general, with the same cross-sectional size and fire exposure, the residual load-bearing capacity of precast concrete columns with cluster reinforcement was greater than that of the other two types of columns. Without severe concrete spalling, the residual load-bearing capacity of precast concrete columns with large-diameter reinforcement was generally similar to that of ordinarily reinforced concrete columns. Specifically, when the fire exposure duration was between 60 and 120 minutes, and the cross-sectional side length was 400 mm, the residual load-bearing capacity of the precast concrete columns with cluster reinforcement was approximately 30% higher than that of the precast concrete columns with large-diameter reinforcement. When the fire exposure duration was 90 minutes, and the cross-sectional side length was 450 mm, the residual load-bearing capacity of the precast concrete columns with cluster reinforcement was up to 40% higher than that of the precast concrete columns with large-diameter reinforcement.

4.2 Residual axial compression stiffness

The change in axial compression stiffness of columns after a fire is an important indicator affecting the deformation performance of the structure. Axial compression stiffness is related to material properties and cross-sectional size. It is defined as the tangent stiffness at 0.4 times of the peak load in the ascending segment of the load-deformation curve.

Formatted: Font: (Default) Times New Roman, (Asian) SimSun

Formatted: Font: (Default) Times New Roman, (Asian) SimSun

Formatted: Font: (Default) Times New Roman, (Asian) SimSun

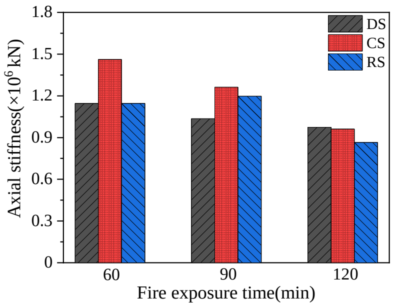

Figure 19 Effect of fire exposure duration on axial compressive stiffness

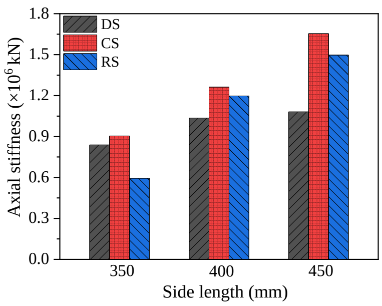

Figure 20 Effect of cross-sectional dimension on axial compressive stiffness

Figure 19~~Figure 19~~ presents the influence of fire exposure duration on the axial compressive stiffness of the concrete columns. As shown, the axial compressive stiffness of the columns decreases as the fire exposure duration increases. This reduction was primarily attributed to the increase in internal concrete temperature with prolonged fire exposure, which intensified dehydration. The originally continuous phase, where cementitious materials were bonded, became a dispersed phase due to the loss of structural water, leading to a reduction in the concrete's elastic modulus and, consequently, a decrease in the axial compressive stiffness of the columns. Compared to 60 minutes of fire exposure, the axial compressive stiffness of the precast concrete columns with large-diameter reinforcement decreased by 10% and 15% after 90 and 120 minutes of fire exposure, respectively. For the precast concrete columns with cluster reinforcement, the axial compressive stiffness decreased by 14% and 34% after 90 and 120 minutes of fire exposure, respectively. This finding suggests that the reduction in axial compressive stiffness is more pronounced in the precast concrete columns with cluster reinforcement than in the precast concrete columns with large-diameter reinforcement.

Formatted: Font: (Default) Times New Roman, (Asian) SimSun

Figure 20~~Figure 20~~ presents the impact of cross-sectional size on the post-fire axial compressive stiffness of the concrete columns. The results indicate that a larger cross-sectional size results in a higher axial compressive stiffness in precast concrete columns after fire exposure. This effect was primarily attributed to the fact that, under the same fire duration, a larger cross-sectional area resulted in a smaller proportion of fire-damaged concrete within the column, thereby reducing stiffness loss. After 90 minutes of fire exposure, comparing with the specimen with cross-sectional side lengths of 350 mm, the axial compressive stiffness of the precast concrete columns reinforced by large-diameter reinforcement with cross-sectional sizes of 400mm and 450mm increased by 24% and 29%, respectively. For the precast concrete columns with cluster reinforcement, the axial compressive stiffness increased by 40% and 83%, respectively. This demonstrated that the increase in cross-sectional size had a more pronounced effect on enhancing the residual axial compressive stiffness of precast concrete columns with cluster reinforcement after fire exposure.

Formatted: Font: (Default) Times New Roman, (Asian) SimSun

Figure 19~~Figure 19~~ and Figure 20~~Figure 20~~ also illustrate the effect of reinforcement configurations on the axial compressive stiffness of concrete columns after fire exposure. For fire durations of 60 and 90 minutes, the residual axial compressive stiffness of the precast concrete columns with cluster reinforcement are greater than the stiffness of the precast concrete columns with large-diameter reinforcement. However, for fire durations of 120 minutes, the stiffness degradation of the precast concrete columns with cluster reinforcement became more pronounced, leading to an axial compressive stiffness that is comparable to the stiffness of the precast concrete columns with large-diameter reinforcement.

Formatted: Font: (Default) Times New Roman, (Asian) SimSun

Formatted: Font: (Default) Times New Roman, (Asian) SimSun

4.3 Residual ductility performance

Ductility refers to the ability of a member to undergo deformation without a significant reduction in load-bearing capacity. It serves as a crucial reference for assessing the deformation capacity of a structure or member. Ductility is measured by the displacement ductility factor μ, which is defined as the ratio of ultimate displacement to yield displacement. The ultimate displacement Δ_u is taken as the displacement corresponding to 0.85 times the peak load on the descending portion of the load-displacement curve, and yield displacement Δ_y is taken as $N_u^T \times L / EA^T$.

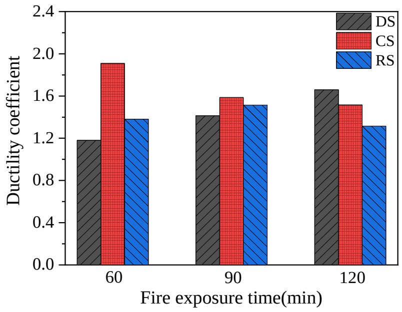

Figure 21 Effect of fire exposure duration on ductility

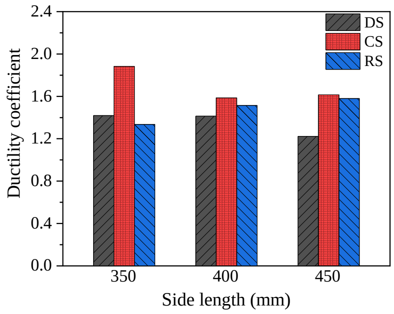

Figure 22 Effect of cross-sectional dimension on ductility

Figure 21~~Figure 21~~ illustrates the effect of varying fire durations on the ductility of concrete columns. For the precast concrete columns with large-diameter reinforcement, an increase in fire exposure duration from 60 to 120 minutes resulted in a higher post-fire ductility. In contrast, the precast concrete columns with cluster reinforcement exhibited the opposite behavior. Figure 22~~Figure 22~~ illustrates the effect of varying cross-sectional sizes on the ductility of concrete columns after exposure to fire. The results indicate that the impact of cross-sectional size on the ductility of post-fire concrete columns is significantly less pronounced compared to its influence on residual strength and stiffness. In general, without the presence of severe concrete spalling, a concrete column with larger cross-sectional size shows reduced post fire ductility.

Figure 21~~Figure 21~~ and Figure 22~~Figure 22~~ further illustrate the influence of different reinforcement configurations on the ductility of concrete columns after fire exposure. The results show that concrete columns with cluster reinforcement exhibit superior ductility compared to the other two reinforcement types. The large-diameter and conventionally reinforced concrete columns feature simpler longitudinal reinforcement layouts with ordinary double-legged stirrups, which provide less effective confinement to the core concrete during failure. In contrast, the precast concrete columns with cluster reinforcement employ composite stirrups to confine the core concrete, resulting in enhanced ductility.

5 Simplified approach for evaluating residual strength of fire-exposed precast concrete column

5.1 Comparison and analysis of existing methods

Several calculation methods for determining residual load-bearing capacity of reinforced concrete columns after fire exposure have been proposed, as summarized in Table 3~~Table 3~~.

Table 3 Methods for calculating residual strength of conventional reinforced concrete columns after fire

Method source	Residual load-bearing capacity calculation formula	Basic principle
Dotreppe et al.[31]	$N_u^T = \gamma\eta\left(\beta_1 f_c A_c + \beta_2 f_y A_s\right)$	Similar to normal temperature load-bearing capacity calculation, but uses numerical calculations to regress the

Formatted: Font: (Asian) SimSun, Not Bold

Formatted: Font: (Asian) SimSun, Not Bold, Pattern: Clear

Formatted: Font: (Asian) SimSun, Not Bold

Formatted: Font: (Asian) SimSun, Not Bold, Pattern: Clear

		high-temperature strength damage coefficient of materials
Xu et al.[28]	$N_{\mathrm{u}}{}^{T} = f_c b^2 \beta_t \beta_L \beta_b \beta_e \beta_\rho \lambda_1 \lambda_2$	Empirical formula directly regressed from numerical calculation results
Eurocode 2[27]	$N_{\mathrm{u}}{}^{T} = A_{core} f_c{}^{T} + A_s f_y{}^{T}$	Similar to normal temperature load-bearing capacity calculation, but accounts for high-temperature damage to concrete by reducing the cross-sectional area

Dotreppe et al.[31] derived a load-bearing capacity formula for reinforced concrete rectangular columns under standard fire conditions through theoretical analysis combined with numerical calculations. This formula considers factors such as fire exposure duration, cross-sectional dimensions, concrete cover thickness, slenderness ratio, eccentricity, and concrete spalling. The equation is presented in Table 3, and the related calculations are shown in reference [31]. Xu et al.[28] developed a numerical model and a computer program, CAFIRE, was written to evaluate the residual load-bearing capacity of reinforced concrete columns after exposure to standard fire. Based on the numerical results, an empirical formula can be obtained by numerical regression to calculate the residual load-bearing capacity of square columns (see Table 3~~Table 3~~). This formula considers also the effects of fire exposure duration, cross-sectional dimensions, effective length, and eccentricity, and is also applicable to biaxial bending [28]. Eurocode 2[27] offers a simplified calculation method based on the 500°C isotherm approach. This method assumes that damaged concrete (i.e., concrete heated above 500°C) does not contribute to the load-bearing capacity, while the remaining concrete retains its initial strength and elastic modulus. The residual load-bearing capacity is thus calculated considering only the cross-sectional area of this remaining concrete. The calculation of this area can be simplified using the method proposed by Kodur[29]. The load-bearing area of the reinforcement remains unchanged, with strength taken as the residual strength after high-temperature exposure. The traditional superposition method can then be used to calculate the post-fire residual load-bearing capacity of reinforced concrete columns, with the formula presented in Table 3, and the related calculations are shown in reference [27].

Table 4~~Table 4~~ presents a comparison of the residual load-bearing capacities calculated using the three methods mentioned above with the experimental results. As shown in the table, the Dotreppe method yields overly conservative predictions. This conservatism primarily stems from the simplified treatment of concrete spalling, by which a reduction factor of 0.85 to the residual load-bearing capacity of columns exposed to fire for more than 30 minutes is applied. However, most of the test columns in this study experienced only minor concrete spalling under fire conditions. The methods proposed by Eurocode 2 and Xu provide relatively more accurate predictions for the residual load-bearing capacities of large-diameter reinforced precast concrete columns and conventional reinforced concrete columns. However, these methods significantly underestimated the residual load-bearing capacity of precast concrete columns reinforced by cluster reinforcement, with the average ratios of calculated to measured values being 0.74 and 0.75, respectively, both with a standard deviation of 0.02. This discrepancy is mainly due to the insufficient consideration of the impact of cluster reinforcement on the columns' residual load-bearing capacity. The cluster reinforcement configuration results in more dispersed placement of longitudinal bars at the four corners of the column's cross-section. After a fire, these dispersed bars effectively increase the load bearing compacity of the damaged concrete. Additionally, the cluster reinforcement requires composite tie bars arranged in a staggered pattern, which provide additional constrains on the damaged concrete and longitudinal bars after the fire. These factors contribute to the delay of the early failure and the increased residual load-bearing capacity of the columns. In conclusion, the comparison results in Table 4~~Table~~

4 indicate that existing calculation methods have certain limitations when they are directly applied to the residual load-bearing capacity calculation of precast concrete columns with efficient reinforcement.

Table 4 Comparison between measured and theoretical calculation values of bearing capacity

Test columns	Column type	Residual capacity (kN)				Ratios		
		Test, N_u^T	Calculated					
			EC2, N_1	Dotreppe, N_2	Xu, N_3	$\frac{N_1}{N_u^T}$	$\frac{N_2}{N_u^T}$	$\frac{N_3}{N_u^T}$
DS-B400-T60	Precast concrete column reinforced by large-diameter reinforcement	4453	4251	3223	4387	0.95	0.72	0.99
DS-B400-T90		4172	3731	2696	3917	0.89	0.65	0.94
DS-B400-T120		3506	3311	2246	3537	0.94	0.64	1.01
DS-B350-T90		3443	2913	1966	3089	0.85	0.57	0.90
DS-B450-T90		4509	4704	3548	4877	1.04	0.79	1.08
CS-B400-T60	Precast concrete columns reinforced by cluster reinforcement	5858	4364	3070	4387	0.74	0.52	0.75
CS-B400-T90		5417	3845	2426	3917	0.71	0.45	0.72
CS-B400-T120		4604	3376	2043	3537	0.73	0.44	0.77
CS-B350-T90		4094	3026	1705	3089	0.74	0.42	0.75
CS-B450-T90		6299	4818	3272	4877	0.76	0.52	0.77
RS-B400-T60	Ordinary reinforced concrete column	3482	4014	3266	4387	1.15	0.94	1.26
RS-B400-T90		3758	3624	2743	3917	0.96	0.73	1.04
RS-B400-T120		3859	3359	2299	3537	0.87	0.60	0.92
RS-B350-T90		2971	2908	2012	3089	0.98	0.68	1.04
RS-B450-T90		4770	4753	3596	4877	1.00	0.75	1.02
				Average		0.89	0.63	0.93
				Standard deviation		0.13	0.14	0.15

5.2 Calculation method for residual load-bearing capacity of the columns with efficient reinforcement

To better account for the enhancement in residual load-bearing capacity of precast concrete columns with cluster reinforcement after a fire, an improved calculation method based on the 500°C isotherm method from Eurocode 2 is proposed. A load-bearing capacity influence factor, α_R, is introduced to consider the effects of different reinforcement configurations. Consequently, the residual load-bearing capacity of precast concrete columns with efficient reinforcement after a fire is calculated using the following equation:

$$N_u^T = \alpha_R \left(A_{c,eff} f_c + A_s f_y^T \right) \tag{1}$$

where: N_u^T is the residual load-bearing capacity of the concrete column after exposure to fire; α_R is the load-bearing capacity adjustment factor, dependent on the reinforcement configuration; $A_{c,eff}$ is the effective cross-sectional area of concrete, which can be calculated using the simplified method proposed by

Kodur[29]; f_c is the compressive strength of concrete at ambient temperature; A_s represents the area of reinforcement; f_y^T is the yield strength of the reinforcement after exposure to fire, as detailed in references[27, 29].

For columns with conventional reinforcement and large-diameter reinforcement, α_R is assumed to be 1. For columns with cluster reinforcement, α_R is set to 1.25 to reflect the enhancement in load-bearing capacity due to the cluster configuration. A comparison between the predicted residual load-bearing capacities of precast concrete columns with efficient reinforcement calculated using the improved method and the experimental values is shown in Figure 23~~Figure 23~~. For precast concrete columns with cluster reinforcement, the ratio of the calculated residual load-bearing capacity to the experimental value had a mean of 0.92 with a standard deviation of 0.02. These results indicate that the improved method provides predictions that align well with the experiments.

Formatted: Font: (Asian) SimSun, Not Bold, Pattern: Clear

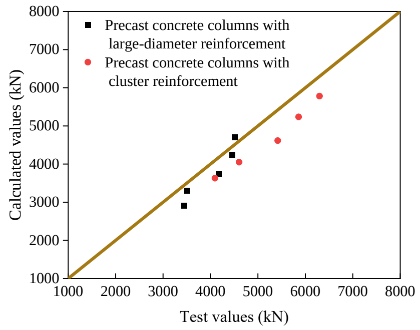

Figure 23 Comparison of calculated and test values of residual load-bearing capacity

6 Conclusions

Based on the standard fire exposure test and residual mechanical behavior tests of 10 precast concrete columns reinforced by efficient reinforcement and 5 conventionally reinforced concrete columns, the following conclusions can be drawn:

(1) Concrete spalling in reinforced concrete columns primarily occurred within the first 30 minutes of the fire. The severity of spalling was positively correlated with the duration of steam generation but showed little correlation with fire exposure duration, reinforcement method, or cross-sectional size. Surface cracks in the concrete widened with increased fire exposure, making them more likely to extend and penetrate.

(2) The temperature distribution on the cross-section of a precast concrete column with efficient reinforcement during fire exposure was similar to that of conventionally reinforced concrete columns, indicating that the reinforcement method had little impact on the temperature field of the section.

(3) The connection zones of precast concrete columns with efficient reinforcement exhibited good performance after fire exposure, with failure typically occurring outside the connection zones.

(4) The residual load-bearing capacity and stiffness of the concrete columns decreased with the increase of fire exposure time. After 60 and 90 minutes of fire exposure, precast concrete columns with cluster reinforcement had higher residual load-bearing capacity, axial compressive stiffness, and ductility than precast concrete columns with large-diameter reinforcement had. However, with further temperature increases, the stiffness of precast concrete columns with cluster reinforcement degraded more significantly, and at 120 minutes, the stiffness of both types of precast concrete columns with efficient reinforcement was nearly the same. The residual

mechanical performance of the conventionally reinforced concrete columns was generally comparable to that of precast concrete columns with large-diameter reinforcement after the fire.

(5) An improved calculation method based on the 500°C isotherm method from Eurocode 2 was proposed. The calculated results showed good agreement with the experimental data, providing a valuable reference for assessing the residual load-bearing capacity of precast concrete columns with efficient reinforcement after a fire.

Acknowledgement

The authors are grateful for the financial support from the National Natural Science Foundation of China (Grant No. 51738011, 51878518) and scientific research fund support from Suzhou City College (Grant No. 3110709223).

References

[1] H Gs. Study on compressive behavior of precast concrete columns with large diameter rebars[D]. Shenyang Jianzhu University,2018.(in Chinese)

[2] L Wh. Experimental study on compressive behavior of precast concrete columns with cluster reinforcement[D]. Shenyang Jianzhu University,2018.(in Chinese)

[3] Y Zhao, R Li, X F Wang, et al. Experimental research on seismic behaviors of precast concrete columns with large-diameter and high-yield strength reinforcements splicing by grout-filled coupling sleeves[J]. China Civil Engineering Journal, 2017(05):27-35.(in Chinese)

[4] Xu L H, Wang Q L, Yu M, et al. Experimental Study On Seismic Behavior of Cluster-Reinforced Precast Concrete Columns with Grouting-Anchor Connections[J]. Journal of Earthquake and Tsunami, 2019,13(03n04):1940007.

[5] Fan J, Feng D, Wu G, et al. Experimental Study of Prefabricated Rc Column-Foundation Assemblies with Two Different Connection Methods and Using Large-Diameter Reinforcing Bars[J]. Engineering Structures, 2020,205:110075.

[6] W Q Y Bin. Numerical Simulation Analysis on Seismic Behavior of Cluster Reinforced Precast Concrete Columns with Grouting — Anchor Connections[J]. Journal of Water Resources and Architectural Engineering, 2019,17(03):66-71.(in Chinese)

[7] X S W T Yang Bin. Experimental investigation and simulation on seismic behavior of prefabricated concrete columns with large diameter and high-yield-strength rebars[J]. Building Structure, 2021,51(S1):744-750.(in Chinese)

[8] Xu H, Yu M, Xue C, et al. Experimental Study On Fire Resistance of Precast Concrete Columns with Efficient Reinforcement[J]. Engineering Structures, 2020,204:109947.

[9] Lie T T, Rowe T J, Lin T D. Residual Strength of Fire-Exposed Reinforced Concrete Columns[J]. Special Publication, 1986,92:153-174.

[10] Lin C, Chen S, Hwang T. Residual Strength of Reinforced Concrete Columns Exposed to Fire[J]. Journal of the Chinese Institute of Engineers, 1989,12(5):557-566.

[11] Lin C H, Tsay C S. Deterioration of Strength and Stiffness of Reinforced Concrete Columns After Fire[J]. Journal of the Chinese Institute of Engineers, 1990,13(3):273-283.

[12] Jau W, Huang K. A Study of Reinforced Concrete Corner Columns After Fire[J]. Cement and Concrete Composites, 2008,30(7):622-638.

[13] Chen Y, Chang Y, Yao G C, et al. Experimental Research On Post-Fire Behaviour of Reinforced Concrete Columns[J]. Fire Safety Journal, 2009,44(5):741-748.

[14] W Bo, L Yihai. Experimental study of the residual axial behavior of axially restrained reinforced concrete columns after fire[J]. China Civil Engineering Journal, 2010,43(4):85-91.(in Chinese)

[15] Z Jiaguang, H Jingsi, X Yan. Experimental study on axial mechanical behavior of reinforced concrete stub columns with pre-load after exposure to high temperatures[J]. JOURNAL OF BUILDING STRUCTURES, 2011,32(4):117-124.(in Chinese)

[16] Z Li-Xin, Y Guang-Lin, J Wen-Liang, et al. Study on the behavior of RC columns with different aggregate after high temperature[J]. Concrete, 2011(1):49-51, 61.(in Chinese)

[17] Mohamed Bikhiet M, El-Shafey N F, El-Hashimy H M. Behavior of Reinforced Concrete Short Columns Exposed to Fire[J]. Alexandria Engineering Journal, 2014,53(3):643-653.

[18] Kodur V, Hibner D, Agrawal A. Residual Response of Reinforced Concrete Columns Exposed to Design Fires[J]. Procedia Engineering, 2017,210:574-581.

[19] Abdulraheem M S, Kadhum M M. Experimental and Numerical Study On Post-Fire Behaviour of Concentrically Loaded Reinforced Reactive Powder Concrete Columns[J]. Construction and Building Materials, 2018,168:877-892.

[20] Abdulraheem M S, Kadhum M M. Experimental Investigation of Fire Effects On Ductility and Stiffness of Reinforced Reactive Powder Concrete Columns Under Axial Compression[J]. Journal of Building Engineering, 2018,20:750-761.

[21] J Chen, J L Wu, Q H Tan, et al. Experimental Study on Mechanical Performance of Reinforced Concrete Stub Columns under and after Fire with Different Restraints[J]. Journal of Disaster Prevention and Mitigation Engineering, 2019,39(03):412-420.(in Chinese)

[22] C Jun, L I Shuai, H Jing-Si, et al. Experimental Study on Axial Mechanical Behavior of Reinforced ConcreteStub Columns after Exposed to the Entire Period of High Temperature[J]. Natural Science Journal of Xiangtan University, 2017,39(2):26-32.(in Chinese)

[23] Huo J, Liu H, Xu X. Effects of Long-Term Loading On Fire-Damaged Reinforced-Concrete Stub Columns[J]. Magazine of Concrete Research, 2019,71(9):476-487.

[24] Huo J, Zhang J, Wang Z, et al. Effects of Sustained Axial Load and Cooling Phase On Post-Fire Behaviour of Reinforced Concrete Stub Columns[J]. Fire Safety Journal, 2013,59:76-87.

[25] Vishal M, Satyanarayanan K S. Experimental Investigation On the Heat Dissipation and Postfire Structural Performance of a Reinforced Concrete Column with Biomimicked Geometry[J]. Fire, 2022,5(6):205.

[26] X K Lin. Experimental study and numerical analysis on residual bearing capacity of reinforced concrete columns after fire[J]. Building Science, 2024,40(05):78-88.(in Chinese)

[27] Eurocode 2: Design of Concrete Structures-Part 1-2:General Rules-Structural Fire Design[S]. Brussels: CEN, 2004.

[28] Y Y Xu, Q F Wang. Research On Residual Strength of Reinforced Concrete Columns After Exposure to Fire[J]. Engineering Mechanics, 2010,27(2):84-89.(in Chinese)

[29] Kodur V K R, Raut N K, Mao X Y, et al. Simplified Approach for Evaluating Residual Strength of Fire-Exposed Reinforced Concrete Columns[J]. Materials & Structures, 2013,46(12):2059-2075.

[30] ISO 834： 1975. Fire Resistance Tests-Elements of Building Construction[S]. Switzerland: International Organization for Standardization, 1975.

[31] Dotreppe J C, Franssen J M, Vanderzeypen Y. Calculation Method for Design of Reinforced Concrete Columns Under Fire Conditions[J]. Aci Structural Journal, 1999,96(1):9-18.